Simulations of HIV Capsid Protein Dimerization Reveal the Effect of Chemistry and Topography on the Mechanism of Hydrophobic Protein Association

Naiyin Yu and Michael F. Hagan*
Martin Fisher School of Physics, Brandeis University, Waltham, Massachusetts

ABSTRACT Recent work has shown that the hydrophobic protein surfaces in aqueous solution sit near a drying transition. The tendency for these surfaces to expel water from their vicinity leads to self-assembly of macromolecular complexes. In this article, we show with a realistic model for a biologically pertinent system how this phenomenon appears at the molecular level. We focus on the association of the C-terminal domain (CA-C) of the human immunodeficiency virus capsid protein. By combining all-atom simulations with specialized sampling techniques, we measure the water density distribution during the approach of two CA-C proteins as a function of separation and amino acid sequence in the interfacial region. The simulations demonstrate that CA-C protein-protein interactions sit at the edge of a dewetting transition and that this mesoscopic manifestation of the underlying liquid-vapor phase transition can be readily manipulated by biology or protein engineering to significantly affect association behavior. Although the wild-type protein remains wet until contact, we identify a set of in silico mutations, in which three hydrophilic amino acids are replaced with nonpolar residues, that leads to dewetting before association. The existence of dewetting depends on the size and relative locations of substituted residues separated by nanometer length scales, indicating long-range cooperativity and a sensitivity to surface topography. These observations identify important details that are missing from descriptions of protein association based on buried hydrophobic surface area.

INTRODUCTION

The hydrophobic effect provides a crucial driving force for the self-assembly of proteins into many biological complexes, such as viral protein coats or capsids (1,2), cytoskeletal filaments (3), and amyloid fibrils (e.g., (4,5)). Although the surfaces of unassembled proteins are wet in solution (6,7), assembly leads to contact surfaces that are dry (8,9). It has been recently shown that hydrophobic protein surfaces sit near a local drying transition, enabling them to form soft interfaces with water that lead to assembly. This work shows how this phenomenom arises in a realistic model.

Many models for self-assembly and other biological association phenomena assume that binding energy is correlated to buried hydrophobic surface area (e.g. (10–12)). Although this generalization has been extremely useful, its accuracy is limited because it does not account for effects such as surface roughness (13), curvature (14,15), or long-range correlations between chemical groups (16). Corrections arising from these effects will be most important for weak protein-protein interactions, which are ubiquitous in biological systems (17) and often essential for the formation of biological assemblages (e.g. (1,18)). By accounting for the molecularity of water, our study provides critical details missing from the surface area-based calculation that elucidate how the geometric arrangement and sizes of different chemical groups within a hydrophobic surface determine its interaction.

Theoretical work (19–21) has shown that hydrophobic association depends on the fact that solvation of a hydrophobic particle exceeding 1 nm in diameter leads to an excess of unsatisfied hydrogen bonds in the surrounding water, which can lead to a state that is close to the liquid-vapor coexistence at ambient conditions. A large, ideal hydrophobic surface (which experiences only repulsive excluded volume interactions with water) pushes the system over a dewetting transition and a liquid-vapor interface is formed (19–21). On the other hand, realistic surfaces such as proteins exert van der Waals and/or electrostatic interactions that attract the water and thus remain wet. The proximity of a dewetting transition is then only revealed by fluctuations of water density (22) or the response of water density to perturbations (15,21), such as the confinement introduced by the approach of two such surfaces. If the surfaces are sufficiently close to a dewetting transition, their approach within a critical distance can lead to dewetting and subsequent hydrophobic collapse (20,21,23–31). However, surfaces of typical proteins found in biological assemblages are geometrically rough and chemically heterogeneous, invariably including hydrophilic groups that locally stabilize liquid water (16,29,31–33). It is unclear how the principles describing dewetting of idealized surfaces can be applied to more complex protein surfaces.

Recently, Patel and co-workers developed specialized sampling techniques (22,34) to measure water density fluctuations in the vicinity of topographically rugged interfaces, and used these to demonstrate that the model proteins BphC and melittin are close to dewetting transition boundaries (31). Here, we apply these techniques to understand the

Submitted June 7, 2012, and accepted for publication August 6, 2012.

*Correspondence: hagan@brandeis.edu

Editor: Josh Wand.

0006-3495/12/09/1363/7 $2.00

http://dx.doi.org/10.1016/j.bpj.2012.08.016

association of the C-terminal domain of the human immunodeficiency virus (HIV) capsid protein (CA-C), as a model system with which to understand the assembly of macromolecular complexes. The size and composition of residues in the interface is typical for protein association interfaces. Furthermore, the CA-C dimerization interface (Fig. 1) plays an essential role in HIV capsid assembly (35–40) and recent studies suggest that it could be a highly effective target for small drug molecules that inhibit assembly (41–43). Isolated CA-C domains dimerize in solution with a dissociation constant of ~10 μM (44) which is similar to that of the full-length CA (18 μM (45)), with structures that closely correspond to those found in mature HIV capsids (39).

We find that, although density fluctuations are enhanced with respect to those found in bulk solution, a dewetting transition does not occur during association of the wild-type (WT) protein. However, the system is close to dewetting as revealed by its sensitivity to perturbations in chemistry or topography. By performing a systematic series of in silico mutations, we identify a set of three hydrophilic residues whose simultaneous mutation to nonpolar amino acids of similar size leads to dewetting during association.

The distances between mutated residues show cooperative effects on nanometer-length scales, whereas the dependence of dewetting on the size of the substituting residues indicates that both topography and chemistry control water behavior. These results indicate that the proximate dewetting transition can be manipulated by small perturbations to the CA-C interfacial microarchitecture to effect large changes in association behavior. In contrast to the assumptions underlying traditional surface-area-based estimates of protein association behavior, our results show that the transition to dewetting does not depend only on the total buried hydrophobic surface area or the mean hydrogen-bonding potential of the surface, but does depend sensitively on the relative locations and sizes of the mutated residues.

System

We perform simulations based on the crystal structure PDBID 1A43 (46), whose electron density closely fits that found at the hexamer-pentamer interface in electron micrographs of the mature HIV capsid structure (39). As shown in Fig. 1, dimerization occurs via the mutual association of α-helix 2 (residues S178–V191). The interface involves ~1200 Å^2 of buried solvent accessible area contributed by nonpolar residues, comprising a hydrophobic "patch" at the center of the contact region, which exceeds a nanometer in all directions. The CA-C dimerization interface is thus representative of capsid protein assembly interfaces and other protein-protein association surfaces in terms of structure and composition. Based on the changes in binding affinity upon mutations of each residue at the dimerization interface, association is primarily driven by hydrophobic interactions but attenuated by electrostatic effects (45,47–51). In particular, residues whose mutation to alanine significantly impair association are mostly nonpolar, whereas mutation of several polar or charged residues (Ser-178, Glu-180, Gln-192) lead to a stronger association (48).

RESULTS

The CA-C interface on an isolated monomer is wet in solution but leads to enhanced water density fluctuations

We began by investigating the behavior of water near the dimerization interface of an isolated WT CA-C monomer. Because the protein surface has an irregular shape, we employed an extension of the indirect umbrella sampling method (34,31) that allows sampling the probability distribution $P_v(N)$ of numbers of water N in an arbitrarily shaped volume v (31) as described in the Methods (in the Supporting Material). As shown in Fig. 2, the mean number of

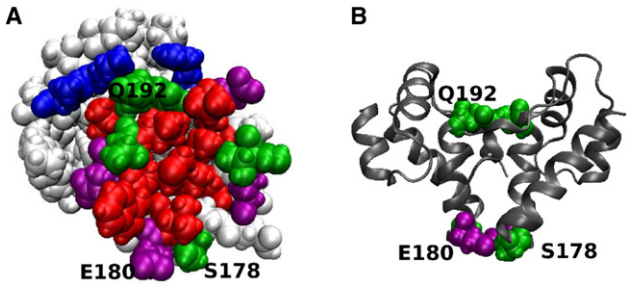

FIGURE 1 Geometry and chemistry of the CA-C dimerization interface. (*A*) A space-filling model of one monomer from the CA-C dimer (PDBID 1A43 (46)). The residues that play a significant role in dimerization ((47)) are color-coded according to residue-type: nonpolar in red, polar in green, basic in blue, and acidic in purple. Three residues that play a key role in determining water behavior, Ser-178, Glu-180, and Gln-192 are labeled. (*B*) A side view of the dimer interface is shown, with Ser-178, Glu-180, and Gln-192 represented by space-filling models and the remainder of CA-C dimer structure shown in ribbon representation. Images created with VMD ((76)).

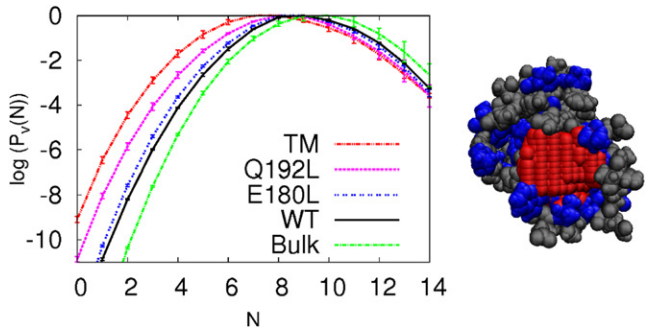

FIGURE 2 Effect of interfacial chemistry on water behavior near isolated CA-C monomers. The distribution of water density fluctuations $P_v(N)$ is shown as a function of the number of waters N in the evaluation volume v (*pictured on the right in red*) in the vicinity of the CA-C dimerization interface. Distributions are shown for WT monomers, monomers with the indicated sets of mutations: E180L, Q192L, and S178A/E180L/Q192L (TM), and a region of bulk water with the same volume as the evaluation region.

waters is close to that found in a region of bulk water with the same volume, reflecting the fact that the surface is wet. However, fluctuations to low densities are enhanced near the interface; i.e., $P_v(N)$ is enhanced at low N in comparison to the distribution for bulk water. This result is consistent with observations on self-assembled monolayers and model proteins BphC and melittin (31).

To understand how water near the interfacial surface responds to perturbations in the protein sequence, we measured $P_v(N)$ in the same volume for CA-C monomers with hydrophilic amino acids in the interfacial region mutated to hydrophobic amino acids with similar sizes. The measured distributions are shown in Fig. 2 for proteins with one to three such mutations. As shown in Fig. 2, the single point mutations lead to a small enhancement of low-N fluctuations, and as additional amino acids are mutated the low-N fluctuations are further enhanced. However, the most probable number of waters in the region changes only slightly, and in all cases the surfaces remain wet. This observation reflects the fact that changing the hydrophobicity of a surface does not affect the mean water density in its vicinity, but rather alters the local water fluctuation behavior.

Water density fluctuations during association

To investigate the behavior of water as two CA-C proteins associate, we placed two monomers at different separation distances D, and calculated $P_v(N)$ in the interfacial region between the monomers (Fig. 3 *A*). Although low-N fluctuations and the probability of drying, $P_v(0)$, increase as the WT monomers approach (Fig. 3 *B*), the interface remains wet until the two surfaces come into contact. Specifically, although the most probable value of N decreases with the monomer separation because the interfacial volume decreases, the mean density remains essentially constant and the most probable value of N remains finite. Thus, we conclude that dimerization of WT CA-C proteins does not involve a dewetting transition.

We next systematically investigated the effect of the interfacial composition on water behavior during association by measuring $P_v(N)$ distributions at a separation of $D = 4$ Å for a series of mutations to amino acids in the interfacial region (Fig. 4). We identified no single point or double mutation that led to a dewetting transition, but the mutation Q192L lead to a significant enhancement of low-N fluctuations (Fig. 4 *A*). We also identified a double mutation, E180L/S178A, for which ~5 waters tend to vacate the interfacial region, but dewetting remains relatively improbable. In contrast, the triple mutation S178A/E180L/Q192L (denoted TM) does lead to dewetting, with a dramatic change in $P_v(N)$ and a most probable value of $N = 0$ (Fig. 4 *B*). A further mutation S178A/E180L/E187L/Q192L (denoted QM) leads to more aggressive dewetting, as indicated by a higher relative probability of $P_v(0)$.

To identify the threshold distance D_t for dewetting during approach of these mutants, we calculated $P_v(N)$ for a series of separation distances D. As shown in Fig. 3 *C*, the surfaces remain wet for distances larger than $D_t \approx 4.1$ Å. Near the critical value, the $P_v(N)$ distributions are bimodal, with high probabilities for the wet (high N) and dry (low N) states separated by a low probability intermediate region, suggesting the presence of a small barrier to dewetting. In a molecular dynamics simulation with two QM monomers held fixed at this separation but no water biasing potential applied to the interfacial region, we observed transitions between locally wet and locally dry states with an approximate timescale of 15 ps. This observation is consistent with the observed barrier size of only a few k_BT and a characteristic timescale for water motions of ~1 ps. A barrier to desolvation could potentially influence the kinetics of dimerization; however, it would be important to determine if such a barrier exists when the proteins associate via different approach vectors.

Dependence of dewetting on the location of mutations

Comparison of $P_v(N)$ from various protein sequences indicates that mutations are cooperative and that the effect

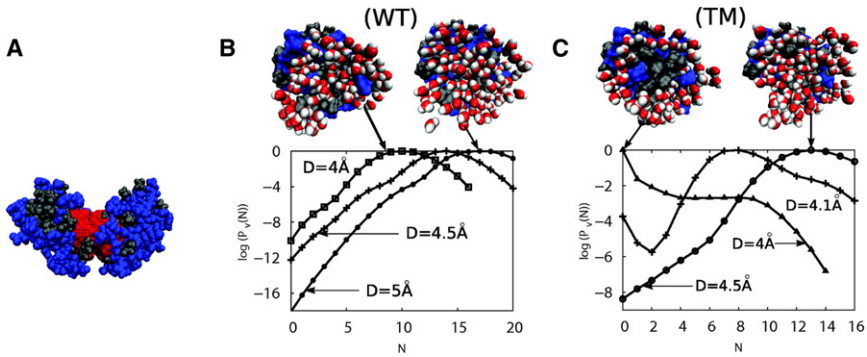

FIGURE 3 Water density distributions during association of CA-C and a mutant. (*A*) The evaluation volume v in red is superposed on the CA-C structure with separation $D = 5$ Å. (*B*) The distribution of water density fluctuations $P_v(N)$ is shown for WT CA-C proteins at separations of $D = 4$, 4.5, and 5 Å. (*C*) The distribution of water density fluctuations $P_v(N)$ is shown during the approach of two S178A/E180L/Q192L (TM) proteins at separations of $D = 4$, 4.1, and 4.5 Å. For *B* and *C*, representative snapshots are shown in which water within 5 Å of both proteins is shown along with one monomer oriented to view the interface in cross section; the solvent accessible surface of the protein is shown, with polar regions colored blue and nonpolar regions colored gray.

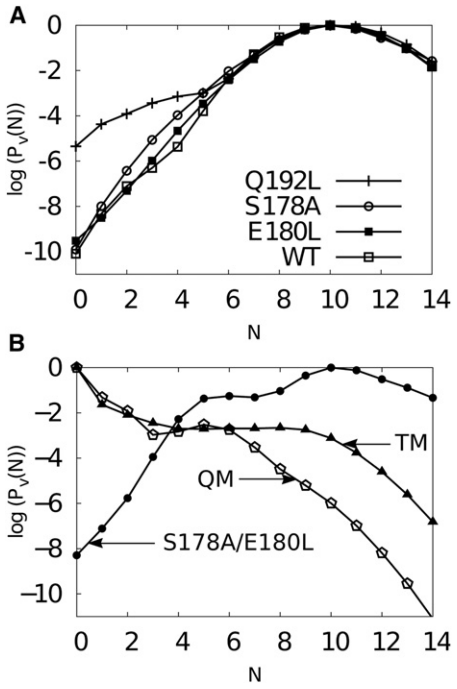

FIGURE 4 Interfacial chemistry determines water behavior during association. The distribution of water density fluctuations $P_v(N)$ is shown for a separation of $D = 4$ Å for (*A*) WT CA-C proteins and indicated single mutations, and (*B*) the indicated sets of multiple mutations.

depends sensitively on the relative location of mutated residues. For example, E180L/S178A increases the probability of evacuating five waters, but the individual mutations E180L and S178A lead to essentially no enhancement of low-*N* fluctuations in comparison to the association of WT proteins. This observation can be understood by noting that the two monomers are rotated by 180 with respect to each other in the crystal structure, meaning that E180 from monomer A is juxtaposed with S178 in monomer B. Thus, the overlapping hydrophobic area increases only if both amino acids are mutated. On the other hand, the single point mutation Q192L does enhance low-*N* fluctuations because the Q192 residues from the two monomers partially overlap in the associated structure. A combination of these three mutations (TM) then leads to a sufficient increase in the contiguous overlapping hydrophobic area to give rise to dewetting, even though the mutated amino acids are separated by up to 10 Å. In contrast, other combinations of three mutations that did not lead to as significant a change in the overlapping hydrophobic area did not lead to dewetting. Similarly, Q192L/E180L did not enhance low-*N* fluctuations of the associating monomers relative to those of Q192L. We thus conclude that perturbations that increase the hydrophobic area of an individual monomer have relatively little effect on the propensity for dewetting during association unless the contiguous overlapping hydrophobic area is increased by the mutation.

Dependence of dewetting on the volume of substituted amino acids

The mutations described in the preceding paragraph were designed to substitute nonpolar amino acids that matched the size and shape of WT residues as closely as possible. However, the contribution of a particular amino acid or group of amino acids to association is commonly assessed experimentally by substitution to alanine, and the most closely related set of mutations that has been studied experimentally is S178A/E180A/E187A/Q192A (QM-A) (48). Given the sensitivity of dewetting to the location of mutations and other small perturbations, we anticipated that the identity of the residue that is substituted for the WT amino acid could also affect water behavior. Thus we repeated our measurements for triple and quadruple mutants in which all residues were substituted with ALA: S178A/E180A/Q192A (TM-A) and QM-A. As shown in Fig. 5, the behavior of these proteins is markedly different from that of TM and QM. Both all-ALA mutation sets exhibit $P_v(N)$, which are similar to those of the WT, and dewetting is not favorable at any separation distance. This observation can be understood by noting that the substituted alanine residues contribute little nonpolar surface area and their small size in comparison to the WT residues decreases the topographic complementarity of the associating interfaces.

Hydrogen bonding potential does not imply propensity for dewetting

It is important to note that the mutations QM and TM do not lead to dewetting simply because they reduce hydrogen bonding between the dimerization interface and solvent, thereby reducing the enthalpic barrier to releasing waters during drying. Both the size-preserving mutants (TM and QM) and the all-alanine mutants (TM-A and QM-A) replace the same number of hydrophilic groups at the interface, and thus should lead to an equivalent reduction in the number of

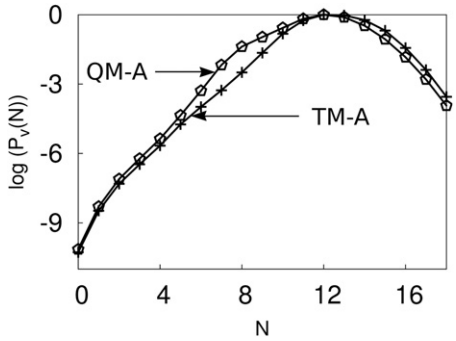

FIGURE 5 Distribution of water density fluctuations $P_v(N)$ is shown for $D = 4$Å from mutants Q192A/E180A/S178A (TM-A) and Q192A/E180A/S178A/E187A (QM-A). The smaller volume of the substituted ALA residues slightly increases the evaluation volume, leading to a larger mean number of waters than observed for WT (Fig. 4 *A*).

hydrogen bonds between the solvated protein interface and water. To verify this supposition, we measured the number of hydrogen bonds among interfacial side chains and water molecules for the cases of isolated monomers (Mon), the dimer complex (Dim), and monomers separated by 4 Å but solvated (Dim-Sol), for the sequences WT, TM, and TM-A. As shown in Table 1, the number of hydrogen bonds is reduced by the same amount within statistical error for both TM and TM-A as compared to WT. The similarity in hydrogen bonding between TM and TM-A, combined with the observation that TM undergoes a dewetting during association, whereas TM-A does not suggests that hydrogen bonding potential and the propensity for dewetting are not uniquely related. Because the shape of the dimer interface is better perserved in TM proteins, we conclude that the geometric complementarity of hydrophobic regions on association surfaces also plays an important role.

DISCUSSION

Our computational prediction of mutations that alter the CA-C association mechanism could be examined by solution measurement of binding affinities for mutated CA-C proteins or the assembly behavior of mutated full-length protein. The existence of dewetting implies a stronger hydrophobic contribution to the association free energy as compared to cases without dewetting. Therefore, we expect that S178A/E180L/Q192L (TM) or S178A/E80L/E187L/Q192L (QM) should have substantially smaller values of K_d than the WT CA-C. Notably, comparison of water behavior for the double mutant S178A/E180L and the mutants S178A/E180L/Q192L (TM) or S178A/E180L/E187L/Q192L (QM) (Fig. 4) shows cooperative effects on water behavior of mutations that are separated by >10 Å.

TABLE 1 Number of hydrogen bonds for interfacial residues of the WT, S178A/E180L/Q192L (TM), and S178A/E180A/Q192A (TM-A) sequences in the case of a solvated monomer (Mon), the dimer complex (Dim), and the two monomers at the verge of association, separated by 4 Å but solvated (Dim-Sol)

		Number of h-bonds	
Configuration	Protein	Waters	Waters and side chains
Mon	WT	32	49
	TM	22	39
	TM-A	22	40
	WT	26	54
Dim	TM	19	43
	TM-A	21	45
	WT	33	52
Dim-Sol	TM	20	40
	TM-A	23	41

Table shows the average number of hydrogen bonds between side chains of the interfacial residues and (column 3) water or (column 4) water and side-chain atoms. The standard error is ~2 hydrogen bonds. The interfacial residues are T148, I150, L151, D152, R154, L172, E175, S178, E180, V181, W184, M185, E187, T188, L189, V191, Q192, N193, K199, and K203.

This cooperativity arises because the protein interface is already situated at the edge of a dewetting transition. Such a result could be surprising, given that effects of mutations, as measured by the resulting change in an association constant, are usually additive over distances of 6 Å or more (52).

Such a comparison is complicated because the mutations will increase the binding affinity by alleviating some repulsion between charged groups in the dimer. For example, the single point mutations S178A, E180A, E187A, and Q192A all led to an increase in the dimerization affinity, likely by eliminating electrostatic repulsions in the dimer (47,48). This complication could be avoided by comparing dissociation constants for the triple or quadruple mutants with the analogous alanine scanning mutants, TM vs. S178A/E180A/Q192A (TM-A) or QM *vs.* S178A/E180A/E187A/Q192A (QM-A). Because repulsions between charged groups are eliminated in both cases, we anticipate that the size and shape preserving mutants TM and QM will have increased dimerization affinities in comparison to TM-A and QM-A. Interestingly, the binding affinity has already been measured for QM-A and the results showed long-range nonadditive effects of the mutations, with a smaller increase in dimerization affinity than for Q192A alone (48).

Notably, the amino acids, which we have found to most strongly influence dewetting, S178, E180, Q192, are highly conserved among HIV and simian immunodeficiency virus (SIV) variants (53) because they are not necessary for stereospecific binding (see Methods in the Supporting Material and (48)). Experimental and theoretical investigations have shown that capsid assembly reactions become trapped when protein-protein interactions are too strong (1,18,54–60). It is possible that the CA-C interface has evolved to avoid a dewetting transition to maintain the relatively weak interactions required for successful assembly.

Because the CA-C dimerization interface is typical of protein binding surfaces, our results raise the possibility that many proteins sit near a dewetting transition. This scenario is consistent with the idea that biological systems tend to position themselves near phase transitions to enable sensitive regulation (61). It can be tested by applying the computational methodologies described here to other proteins to identify mutations that bring about or eliminate dewetting during association, and then experimentally investigating the effects of these mutations on binding affinities. Considering the requirement for weak binding interactions in biological assembly reactions and the prevalence of assembly in biological systems, it is of great importance to extend our understanding of the relationship between sequence, structure, and association behavior to include effects of the molecularity of water, as we have done here for CA-C.

SUPPORTING MATERIAL

Methods, two figures, and references (62–76) are available at http://www.biophysj.org/biophysj/supplemental/S0006-3495(12)00878-8.

This work was supported by award No. R01AI080791 from the National Institute Of Allergy And Infectious Diseases. Computational resources were provided by the National Science Foundation through TeraGrid computing resources (LONI Queenbee and SDSC Trestles) and the Brandeis HPCC. We are most grateful to Patrick Varilly for providing us with a patch to perform INDUS sampling in GROMACS, to David Chandler for comments on manuscript, and to Francesco Pontiggia for insightful discussions.

REFERENCES

1. Ceres, P., and A. Zlotnick. 2002. Weak protein-protein interactions are sufficient to drive assembly of hepatitis B virus capsids. *Biochemistry.* 41:11525–11531.
2. Kegel, W. K., and P. Schoot Pv. 2004. Competing hydrophobic and screened-coulomb interactions in hepatitis B virus capsid assembly. *Biophys. J.* 86:3905–3913.
3. Vulevic, B., and J. J. Correia. 1997. Thermodynamic and structural analysis of microtubule assembly: the role of GTP hydrolysis. *Biophys. J.* 72:1357–1375.
4. Paravastu, A. K., R. D. Leapman, …, R. Tycko. 2008. Molecular structural basis for polymorphism in Alzheimer's beta-amyloid fibrils. *Proc. Natl. Acad. Sci. USA.* 105:18349–18354.
5. Sachse, C., M. Fändrich, and N. Grigorieff. 2008. Paired beta-sheet structure of an Abeta(1–40) amyloid fibril revealed by electron microscopy. *Proc. Natl. Acad. Sci. USA.* 105:7462–7466.
6. Cheng, Y.-K., and P. J. Rossky. 1998. Surface topography dependence of biomolecular hydrophobic hydration. *Nature.* 392:696–699.
7. Zhou, R., X. Huang, …, B. J. Berne. 2004. Hydrophobic collapse in multidomain protein folding. *Science.* 305:1605–1609.
8. Larsen, T. A., A. J. Olson, and D. S. Goodsell. 1998. Morphology of protein-protein interfaces. *Structure.* 6:421–427.
9. Rodier, F., R. P. Bahadur, …, J. Janin. 2005. Hydration of protein-protein interfaces. *Proteins.* 60:36–45.
10. Eisenberg, D., and A. D. McLachlan. 1986. Solvation energy in protein folding and binding. *Nature.* 319:199–203.
11. Spolar, R. S., and M. T. Record, Jr. 1994. Coupling of local folding to site-specific binding of proteins to DNA. *Science.* 263:777–784.
12. Horton, N., and M. Lewis. 1992. Calculation of the free energy of association for protein complexes. *Protein Sci.* 1:169–181.
13. Mittal, J., and G. Hummer. 2010. Interfacial thermodynamics of confined water near molecularly rough surfaces. *Faraday Discuss.* 146:341–352, discussion 367–393; 395–401.
14. Hummer, G., and S. Garde. 1998. Cavity expulsion and weak dewetting of hydrophobic solutes in water. *Phys. Rev. Lett.* 80:4193–4196.
15. Huang, D. M., and D. Chandler. 2000. Temperature and length scale dependence of hydrophobic effects and their possible implications for protein folding. *Proc. Natl. Acad. Sci. USA.* 97:8324–8327.
16. Acharya, H., S. Vembanur, …, S. Garde. 2010. Mapping hydrophobicity at the nanoscale: applications to heterogeneous surfaces and proteins. *Faraday Discuss.* 146:353–365, discussion 367–393; 395–401.
17. Nooren, I. M. A., and J. M. Thornton. 2003. Diversity of protein-protein interactions. *EMBO J.* 22:3486–3492.
18. Zlotnick, A. 2003. Are weak protein-protein interactions the general rule in capsid assembly? *Virology.* 315:269–274.
19. Stillinger, F. H. 1973. Structure in aqueous solutions of nonpolar solutes from the standpoint of scaled-particle theory. *J. Solution Chem.* 2:141–158.
20. Lum, K., D. Chandler, and J. D. Weeks. 1999. Hydrophobicity at small and large length scales. *J. Phys. Chem. B.* 103:4570–4577.
21. Chandler, D. 2005. Interfaces and the driving force of hydrophobic assembly. *Nature.* 437:640–647.
22. Patel, A. J., P. Varilly, and D. Chandler. 2010. Fluctuations of water near extended hydrophobic and hydrophilic surfaces. *J. Phys. Chem. B.* 114:1632–1637.
23. Lee, C.-Y., J. A. McCammon, and P. J. Rossky. 1984. The structure of liquid water at an extended hydrophobic surface. *J. Chem. Phys.* 80:4448–4455.
24. Parker, J. L., P. M. Claesson, and P. Attard. 1994. Bubbles, cavities, and the long-ranged attraction between hydrophobic surfaces. *J. Phys. Chem.* 98:8468–8480.
25. Carambassis, A., L. C. Jonker, …, M. W. Rutland. 1998. Forces measured between hydrophobic surfaces due to a submicroscopic bridging bubble. *Phys. Rev. Lett.* 80:5357–5360.
26. Christenson, H. K., and P. M. Claesson. 2001. Direct measurements of the force between hydrophobic surfaces in water. *Adv. Colloid Interface Sci.* 91:391–436.
27. Berne, B. J., J. D. Weeks, and R. Zhou. 2009. Dewetting and hydrophobic interaction in physical and biological systems. *Annu. Rev. Phys. Chem.* 60:85–103.
28. Liu, P., X. Huang, …, B. J. Berne. 2005. Observation of a dewetting transition in the collapse of the melittin tetramer. *Nature.* 437:159–162.
29. Giovambattista, N., C. F. Lopez, …, P. G. Debenedetti. 2008. Hydrophobicity of protein surfaces: separating geometry from chemistry. *Proc. Natl. Acad. Sci. USA.* 105:2274–2279.
30. Krone, M. G., L. Hua, …, J. E. Shea. 2008. Role of water in mediating the assembly of Alzheimer amyloid-beta Abeta16-22 protofilaments. *J. Am. Chem. Soc.* 130:11066–11072.
31. Patel, A. J., P. Varilly, …, S. Garde. 2012. Sitting at the edge: how biomolecules use hydrophobicity to tune their interactions and function. *J. Phys. Chem. B.* 116:2498–2503.
32. Hua, L., R. Zangi, and B. J. Berne. 2009. Hydrophobic interactions and dewetting between plates with hydrophobic and hydrophilic domains. *J. Phys. Chem. C.* 113:5244–5253.
33. Koishi, T., K. Yasuoka, …, X. C. Zeng. 2005. Large-scale molecular-dynamics simulation of nanoscale hydrophobic interaction and nanobubble formation. *J. Chem. Phys.* 123:204707–204713.
34. Patel, A. J., P. Varilly, …, S. Garde. 2011. Quantifying density fluctuations in volumes of all shapes and sizes using indirect umbrella sampling. *J. Stat. Phys.* 145:265–275.
35. Mateu, M. G. 2009. The capsid protein of human immunodeficiency virus: intersubunit interactions during virus assembly. *FEBS J.* 276: 6098–6109.
36. Ganser-Pornillos, B. K., A. Cheng, and M. Yeager. 2007. Structure of full-length HIV-1 CA: a model for the mature capsid lattice. *Cell.* 131:70–79.
37. Pornillos, O., B. K. Ganser-Pornillos, …, M. Yeager. 2010. Disulfide bond stabilization of the hexameric capsomer of human immunodeficiency virus. *J. Mol. Biol.* 401:985–995.
38. Pornillos, O., B. K. Ganser-Pornillos, …, M. Yeager. 2009. X-ray structures of the hexameric building block of the HIV capsid. *Cell.* 137: 1282–1292.
39. Pornillos, O., B. K. Ganser-Pornillos, and M. Yeager. 2011. Atomic-level modelling of the HIV capsid. *Nature.* 469:424–427.
40. von Schwedler, U. K., K. M. Stray, …, W. I. Sundquist. 2003. Functional surfaces of the human immunodeficiency virus type 1 capsid protein. *J. Virol.* 77:5439–5450.
41. Zhang, J. Y., X. Y. Liu, and E. De Clercq. 2009. Capsid (CA) protein as a novel drug target: recent progress in the research of HIV-1 CA inhibitors. *Mini Rev. Med. Chem.* 9:510–518.
42. Bocanegra, R., M. Nevot, …, M. G. Mateu. 2011. Rationally designed interfacial peptides are efficient in vitro inhibitors of HIV-1 capsid assembly with antiviral activity. *PLoS ONE.* 6:e23877.
43. Dahirel, V., K. Shekhar, …, A. K. Chakraborty. 2011. Coordinate linkage of HIV evolution reveals regions of immunological vulnerability. *Proc. Natl. Acad. Sci. USA.* 108:11530–11535.

44. Mateu, M. G. 2002. Conformational stability of dimeric and monomeric forms of the C-terminal domain of human immunodeficiency virus-1 capsid protein. *J. Mol. Biol.* 318:519–531.

45. Gamble, T. R., S. Yoo, …, C. P. Hill. 1997. Structure of the carboxyl-terminal dimerization domain of the HIV-1 capsid protein. *Science.* 278:849–853.

46. Worthylake, D. K., H. Wang, …, C. P. Hill. 1999. Structures of the HIV-1 capsid protein dimerization domain at 2.6 A resolution. *Acta Crystallogr. D Biol. Crystallogr.* 55:85–92.

47. del Alamo, M., J. L. Neira, and M. G. Mateu. 2003. Thermodynamic dissection of a low affinity protein-protein interface involved in human immunodeficiency virus assembly. *J. Biol. Chem.* 278:27923–27929.

48. del Alamo, M., and M. G. Mateu. 2005. Electrostatic repulsion, compensatory mutations, and long-range non-additive effects at the dimerization interface of the HIV capsid protein. *J. Mol. Biol.* 345:893–906.

49. Alcaraz, L. A., M. Del Alamo, …, J. L. Neira. 2008. Structural mobility of the monomeric C-terminal domain of the HIV-1 capsid protein. *FEBS J.* 275:3299–3311.

50. Ganser-Pornillos, B. K., U. K. von Schwedler, …, W. I. Sundquist. 2004. Assembly properties of the human immunodeficiency virus type 1 CA protein. *J. Virol.* 78:2545–2552.

51. Yu, X., Q. Wang, …, J. Zheng. 2009. Mutational analysis and allosteric effects in the HIV-1 capsid protein carboxyl-terminal dimerization domain. *Biomacromolecules.* 10:390–399.

52. Schreiber, G., and A. R. Fersht. 1995. Energetics of protein-protein interactions: analysis of the barnase-barstar interface by single mutations and double mutant cycles. *J. Mol. Biol.* 248:478–486.

53. Kuiken, C., B. Foley, …, B. Korber, editors. 2010. HIV Sequence Compendium 2010. Theoretical Biology and Biophysics Group, Los Alamos National Laboratory, NM.

54. Endres, D., and A. Zlotnick. 2002. Model-based analysis of assembly kinetics for virus capsids or other spherical polymers. *Biophys. J.* 83: 1217–1230.

55. Hagan, M. F., and D. Chandler. 2006. Dynamic pathways for viral capsid assembly. *Biophys. J.* 91:42–54.

56. Jack, R. L., M. F. Hagan, and D. Chandler. 2007. Fluctuation-dissipation ratios in the dynamics of self-assembly. *Phys. Rev. E Stat. Nonlin. Soft Matter Phys.* 76:021119.

57. Nguyen, H. D., V. S. Reddy, and C. L. Brooks, 3rd. 2007. Deciphering the kinetic mechanism of spontaneous self-assembly of icosahedral capsids. *Nano Lett.* 7:338–344.

58. Rapaport, D. C. 2010. Studies of reversible capsid shell growth. *J. Phys. Condens. Matter.* 22:104115.

59. Hagan, M. F., and O. M. Elrad. 2010. Understanding the concentration dependence of viral capsid assembly kinetics—the origin of the lag time and identifying the critical nucleus size. *Biophys. J.* 98:1065–1074.

60. Hagan, M. F., O. M. Elrad, and R. L. Jack. 2011. Mechanisms of kinetic trapping in self-assembly and phase transformation. *J. Chem. Phys.* 135:104115.

61. Mora, T., and W. Bialek. 2011. Are biological systems poised at criticality? *J. Stat. Phys.* 144:268–302.

62. Hess, B., C. Kutzner, …, E. Lindahl. 2008. GROMACS 4: algorithms for highly efficient, load-balanced, and scalable molecular simulation. *J. Chem. Theory Comput.* 4:435–447.

63. Kaminski, G. A., R. A. Friesner, …, W. L. Jorgensen. 2001. Evaluation and reparametrization of the OPLS-AA force field for proteins via comparison with accurate quantum chemical calculations on peptides. *J. Phys. Chem. B.* 105:6474–6487.

64. Jorgensen, W. L., J. Chandrasekhar, …, M. L. Klein. 1983. Comparison of simple potential functions for simulating liquid water. *J. Chem. Phys.* 79:926–936.

65. Hornak, V., R. Abel, …, C. Simmerling. 2006. Comparison of multiple Amber force fields and development of improved protein backbone parameters. *Proteins.* 65:712–725.

66. Berendsen, H. J. C., J. R. Grigera, and T. P. Straatsma. 1987. The missing term in effective pair potentials. *J. Phys. Chem.* 91:6269–6271.

67. Bjelkmar, P., P. Larsson, …, E. Lindahl. 2010. Implementation of the CHARMM force field in GROMACS: analysis of protein stability effects from correction maps, virtual interaction sites, and water models. *J. Chem. Theory Comput.* 6:459–466.

68. Bussi, G., D. Donadio, and M. Parrinello. 2007. Canonical sampling through velocity rescaling. *J. Chem. Phys.* 126:014101.

69. Miyamoto, S., and P. A. Kollman. 1992. SETTLE - an analytical version of the SHAKE and RATTLE algorithm for rigid water models. *J. Comput. Chem.* 13:952–962.

70. Hess, B., H. Bekker, …, J. G. E. M. Fraaije. 1997. LINCS: a linear constraint solver for molecular simulations. *J. Comput. Chem.* 18: 1463–1472.

71. Essmann, U., L. Perera, …, L. G. Pedersen. 1995. A smooth particle mesh Ewald method. *J. Chem. Phys.* 103:8577–8593.

72. de Berg, M., O. Cheong, …, M. Overmaras. 2008. Computational Geometry: Algorithms and Applications, 3rd ed. Springer.

73. Kumar, S., J. M. Rosenberg, …, P. A. Kollma. 1992. THE weighted histogram analysis method for free-energy calculations on biomolecules. I. The method. *J. Comput. Chem.* 13:1011–1021.

74. Lidón-Moya, M. C., F. N. Barrera, …, J. L. Neira. 2005. An extensive thermodynamic characterization of the dimerization domain of the HIV-1 capsid protein. *Protein Sci.* 14:2387–2404.

75. Alcaraz, L. A., M. del Alamo, …, J. L. Neira. 2007. Flexibility in HIV-1 assembly subunits: solution structure of the monomeric C-terminal domain of the capsid protein. *Biophys. J.* 93:1264–1276.

76. Humphrey, W., A. Dalke, and K. Schulten. 1996. VMD: visual molecular dynamics. *J. Mol. Graph.* 14:33–38, 27–28.